# Realizing Envisat's potential for rain cloud studies

Graham D. Quartly[1] and Trevor H. Guymer[1]

Received 5 December 2006; revised 2 February 2007; accepted 3 April 2007; published 8 May 2007.

[1] Owing to the highly variable nature of rain both in space and time and the difficulties in obtaining accurate in situ measurements, increasing reliance is being placed on the various types of satellite data now available. The multi-sensor payload of *Envisat* is of particular interest because the data are co-located and simultaneous, thus reducing some of the uncertainty found in multi-platform analyses. This paper shows variations in cloud and precipitation data derived from AATSR, RA-2 and MWR-2 measurements in an overpass of Hurricane Juan, revealing significant asymmetry in the spatial distribution. The results are discussed in the context of similar data from other tropical and sub-tropical features in the western Atlantic. The combination of data from these sensors allows us to see the effects of different drop-size distribution at varying distances from the hurricane's eye and to conclude that active microwave systems are needed for studying small-scale variations in rainfall. **Citation:** Quartly, G. D., and T. H. Guymer (2007), Realizing Envisat's potential for rain cloud studies, *Geophys. Res. Lett.*, *34*, L09807, doi:10.1029/2006GL028996.

## 1. Introduction

[2] The study of storms at sea is important not only for their effect on ocean dynamics, through wind-induced currents, mixing, wave set-up and freshwater input, but also because knowledge of the development of such storms is critical for accurate forecasting of events affecting both shipping and coastal areas. Such a concern became particularly pronounced in 2005, when the North Atlantic produced more tropical storms (27 in all) than in any of the preceding 40 years.

[3] To date, there has been only one satellite, TRMM, dedicated to observing rain systems, but there is a panoply of other sensors producing some quantitative values associated with raining clouds. *Quartly et al.* [2002] summarise how the different components of a large convective cloud system affect the signal detected by various infra-red, optical and microwave sensors.

[4] A problem remains in making use of these different sources of information: since rain systems evolve rapidly, it is difficult to combine observations from different sensors making measurements at different times. NASA has recently overcome this hurdle by placing a number of complementary sensors within the orbital cluster known as the 'A-train'. ESA adopted the alternative approach of placing multiple instruments on a single very large satellite, with *Envisat* being the culmination of this approach. This paper examines the complementarity of three different sensors for studies of marine storms. We confined our search to the western N. Atlantic, and found 10 major rain events (fronts and storms) in Sept/Oct. 2003. Section 2 provides a brief recapitulation on the derivation of quantitative values from the individual sensors; section 3 discusses one particular case study, whilst section 4 characterises the typical relationships found for all the Atlantic events. The final section summarises the findings, and discusses ideas for future developments.

## 2. *Envisat* Instruments

[5] *Envisat* is a large (8000 kg) satellite, hosting 10 different instruments (see http://www.envisat.esa.int/instruments), which was designed for multi-disciplinary applications spanning land, ice, sea and atmosphere. It was launched on 1st Mar. 2002 into an orbit of 98° inclination, giving near-global coverage, and data are routinely made available in near real-time. 'Level 2' data are used here, which are fully quality-controlled, but in principle similar analyses could be implemented on near real-time data.

### 2.1. Radar Altimeter, RA-2

[6] The RA-2 is an active microwave instrument, reflecting pulses of $K_u$-band and S-band radiation from the sea surface. The backscatter strength, $\sigma^0$, corresponds to a footprint size of ~8 km diameter, with both $\sigma^0_{Ku}$ and $\sigma^0_S$ principally responding to changes in surface roughness due to wind. Consequently, there is a tight non-linear empirical relationship, f(.), between them for non-raining conditions [*Quartly and Srokosz*, 2003; *Tournadre and Quartly*, 2003]. However, rain will cause a decrease in the $K_u$-band signal, $\Delta\sigma^0$ (in dB), which is related to rain rate by:

$$\Delta\sigma^0 = \sigma^0_{Ku} - f\left(\sigma^0_S\right) = 2\,H\,a\,R^b \tag{1}$$

where $H$ is the height (in km) of the rain column, $R$ is the rain rate in mm $hr^{-1}$, and $a$ = 0.02038 dB $km^{-1}$ and $b$ = 1.203 [*Goldhirsh and Walsh*, 1982]. The attenuation at S-band is an order of magnitude smaller than at $K_u$-band, but, in principle, changes in the backscatter at the lower (reference) frequency can be determined in an iterative manner [*Quilfen et al.*, 2006].

### 2.2. Microwave Radiometer, MWR-2

[7] The nadir-pointing passive microwave radiometer on *Envisat* operates at two channels (24 and 36 GHz), both with a footprint ~20 km in diameter. The MWR-2 data are used to calculate $\theta$, a set of geophysical estimates and corrections, including liquid water content (LWC) and water vapour (WV), using a neural net, $N$:

$$\theta = N\left(BT_{24}, BT_{36}, \sigma^0_{Ku}\right) \tag{2}$$

[1]National Oceanography Centre, Southampton, UK.


0094-8276/07/2006GL028996

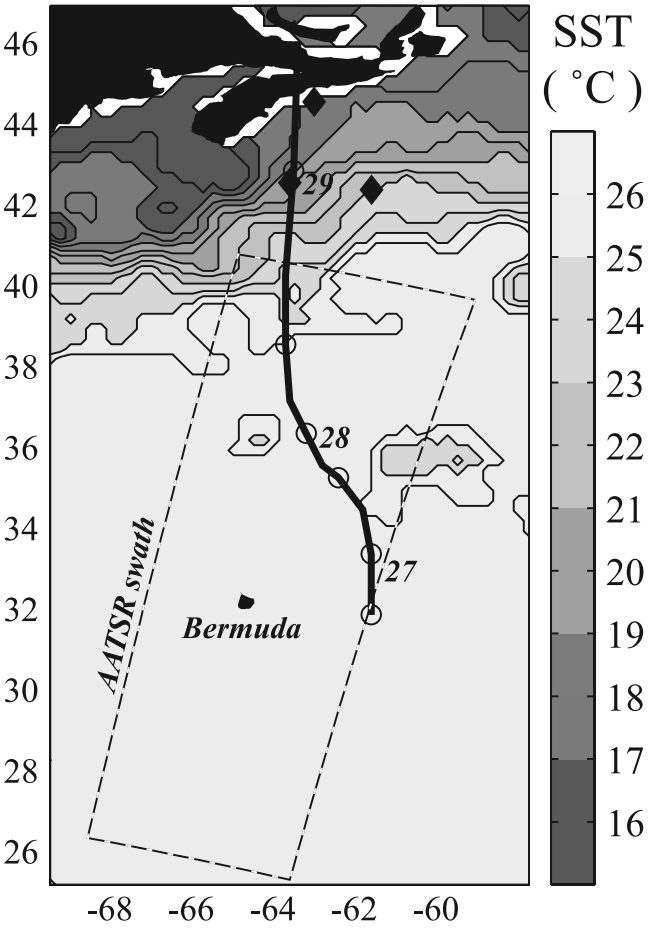


**Figure 1.** Sea surface temperature (SST) in western N. Atlantic on 27th Sept. 2003, with track of Hurricane Juan superimposed (circles mark every 12 hours, with numbers representing position at midday). Diamonds near Nova Scotia mark positions of wave buoys.

where BT are the brightness temperatures, and $\sigma^0_{Ku}$ (the measured backscatter without atmospheric correction) is used to give a measure of surface roughness and hence wave-breaking, which affects surface emissivity. This formulation [*Obligis et al.*, 2006] gives smaller errors than the previous polynomial form. However, as discussed earlier, $\sigma^0_{Ku}$ is not a good measure of surface roughness in rainy conditions, so we use f($\sigma^0_S$) instead. As we will show, this gives much more realistic profiles across storm events; away from these, this substitution only effects estimates of LWC and WV by 4.1% and 0.6% respectively.

### 2.3. Advanced Along-Track Scanning Radiometer, AATSR

[8] The AATSR is a dual-view scanning infra-red radiometer; here we only consider data from near nadir-viewing, which are provided with a resolution of ~1 km. Accurately calibrated brightness temperature data are recorded at wavelengths of 0.55, 0.66, 0.87, 1.6, 3.7, 11, and 12 $\mu$m. The values at the longest five wavelengths are combined with a radiative flux model [*Watts et al.*, 1998] initialised by an atmospheric temperature profile from ECMWF, to produce estimates of cloud fraction, particle size, optical depth and cloud top height. The inversion used here avoids the 12 $\mu$m channel, because the true values at the centre of these intense rain events were lower than the prescribed data range.

[9] Thus between these three multi-frequency sensors, ranging from infra-red to passive and active microwave instruments, *Envisat* has the ability to record many properties of the air column, cloud and attendant rainfall, as well as the metocean parameters of wind speed and wave height.

## 3. Hurricane Juan (Sept. 2003)

### 3.1. Background

[10] Hurricane Juan was selected as a case study because of its unusual characteristics and also because it was overflown by *Envisat* during its 3-day existence as a hurricane (Figure 1). It became associated with a subtropical front, but instead of dissipating as it moved northwards from Bermuda, it strengthened from a tropical storm to a category-2 hurricane — a status it maintained until it made landfall near Halifax, Nova Scotia as the most powerful hurricane to hit the region since 1873. Hurricanes lose energy when the underlying water temperature is less than 26°C; however, Juan maintained its status because temperatures between the Gulf Stream and Nova Scotia were 3–4°C higher than normal [*Fogarty et al.*, 2006], and it crossed that region quickly. On approaching land its translational speed was 15 m $s^{-1}$, which also resulted in much higher surface wind speeds on the eastern side of the storm than would otherwise have been the case. Conversely, the winds on the western flank were much lighter, resulting in a very asymmetric wind field, as observed by *QuikScat* at 22:15 on Sept. 28 (C. Fogarty, Hurricane Juan, available at http://www.novaweather.net/Hurricane_Juan.html, 2003) and by coastal buoys and land stations as Juan made landfall. However, wave heights measured by the buoys shown in Figure 1 appeared to be more symmetrical about the eye, with values peaking at 6–8 m, except for the buoy that encountered the eye wall, which recorded wave heights exceeding 9.5 m for two hours.

[11] Juan also exhibited asymmetry in other ways. Sequences of infra-red imagery from a geostationary meteorological satellite, and data from precipitation radars in Nova Scotia and a reconnaissance aircraft showed that Hurricane Juan was asymmetric in its cloud and precipitation fields (http://www.novaweather.net/Hurricane_Juan.html), with most of the active deep convection confined to the north of the eye.

### 3.2. Analysis of Data From Envisat Pass

[12] *Envisat* overflew Juan at 14:37 UT on 27th Sept., while it was near Bermuda. The two images in Figure 2 are of Cloud Top Height (CTH) and Optical Depth (OD) derived from AATSR, OD being a non-dimensional measure of cloud thickness. Juan is marked by a well-developed, cyclonic pattern to the clouds with a pronounced eye at 35.2°N, 63.0°W. CTH exceeds 12 km over a large area but is asymmetric with respect to the eye, lying mainly to the north and west. A sharp change is found to the south with CTH values decreasing to 2 km in a short distance. This lower height marks the top of boundary layer cumulus typical of the subtropics in the absence of major disturbances. OD has a similar asymmetric distribution with values exceeding 100 in the region of high CTH. Also shown in

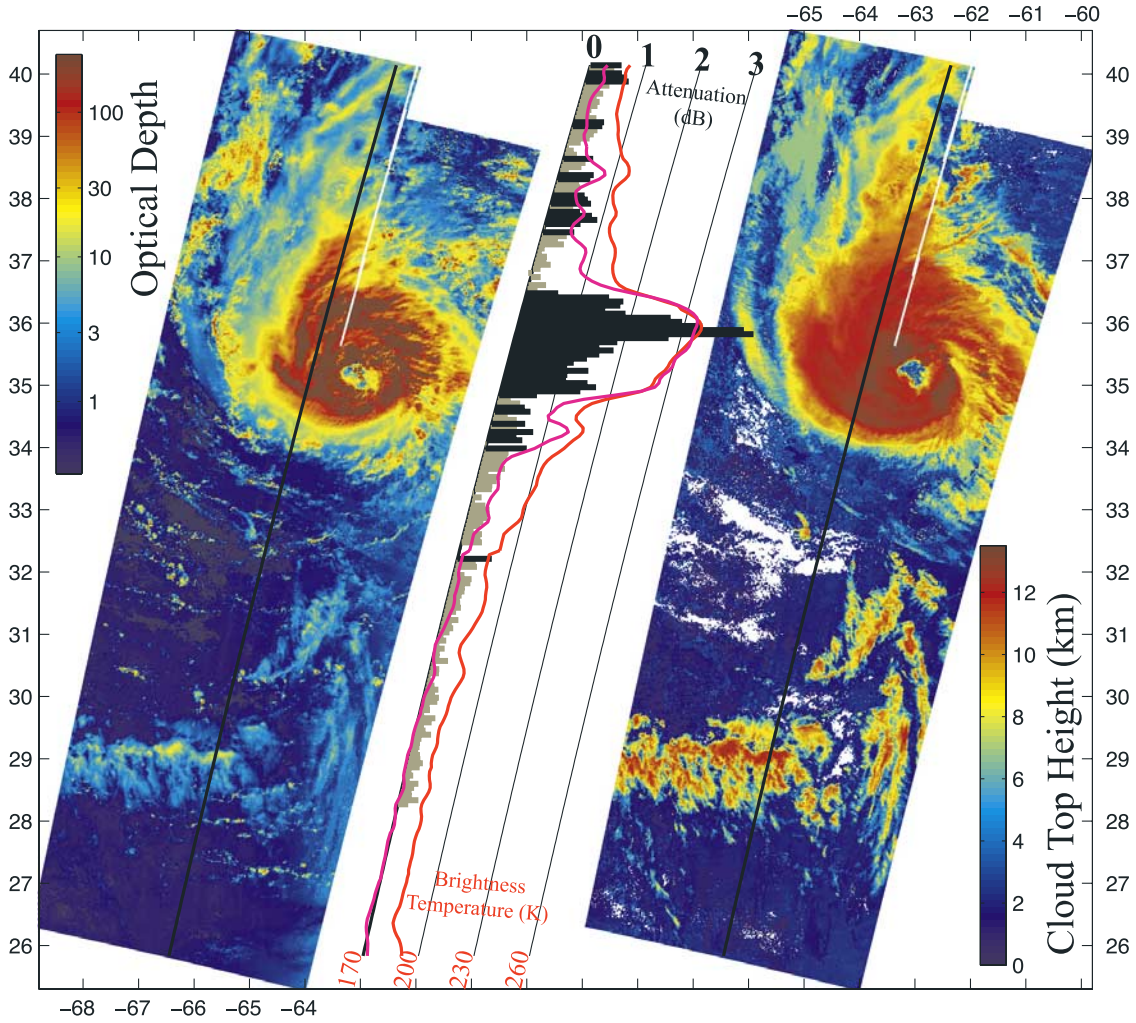


**Figure 2.** Combined sensor output for a single *Envisat* pass across Hurricane Juan at 14:37 UT on 27th Sept. 2003. (left, right) Swath information derived from the AATSR, with the black lines indicating the nadir track. (middle) The derived attenuation from the RA-2 (in black when statistically significant) along with the BT values from the MWR-2 channels (pink 24 GHz, red 36 GHz).

Figure 2 are the variations of radar attenuation from RA-2 and BTs from MWR-2 along the middle of the AATSR swath. High BTs and attenuation tend to be associated with one another and are confined to deep cloud.

[13] The relationship between the AATSR, RA-2 and MWR-derived parameters can be explored by considering a section along the nadir track, the only place where data from all three sensors coincide in space and time (Figure 3). Rain rates derived from the RA-2 exceed 5 mm $hr^{-1}$ within the hurricane, reaching 10 mm $hr^{-1}$ at maximum, and with most of the rain occurring to the north of the eye. Discrete rain regions also occur around 34.2°N and 37.8°N at the edge of the high clouds, with rain rates just above the detection threshold (2.3 mm $hr^{-1}$) also stretching further north. These rates are within the range observed 18 hours later by the land and aircraft-based precipitation radars (http://www.novaweather.net/Hurricane_Juan.html). Altimeter-derived wave heights reached 6 m, consistent with the buoy values (see section 3.1), with the peaks in wind, waves and rain coinciding at ~50 km north of the nearest approach to the eye. Using wind speeds calculated using $f(\sigma^0_S)$ (which is more robust than $\sigma^0_{Ku}$ in rain), we determined the wave heights that would be in equilibrium with the winds [*Pierson and Moskowitz*, 1984]. This shows the central 300 km of the transect to be the only part not fully-developed. (Note, for the TOPEX altimeter the wave height values at the lower frequency (C-band) can be used through storms [*Quartly*, 1997]; those for *Envisat* are too noisy to merit inclusion in Figure 3c.) Within the neural net, the formulation for WV is sensitive to the perceived $\sigma^0$ (Figure 3d), whereas LWC is not (Figure 3e).

[14] The plots of CTH and OD (Figures 3g and 3h) have similar shape. Some parts of the hurricane have OD > 100 which suggests the cloud is not only high but deep, as might be expected in regions of active convection. However, the high cloud at ~29°N has much lower values (OD ~3–10), which may indicate that cloud cover is dominated by cirrus as a remnant of previous (convective or frontal) activity. Moreover, the RA-2 and MWR profiles show no rain or any significant LWC or WV there. MODIS observations just over an hour later show a large area near the centre of Juan where Cloud Top Pressure was less than 250 hPa (equiva-

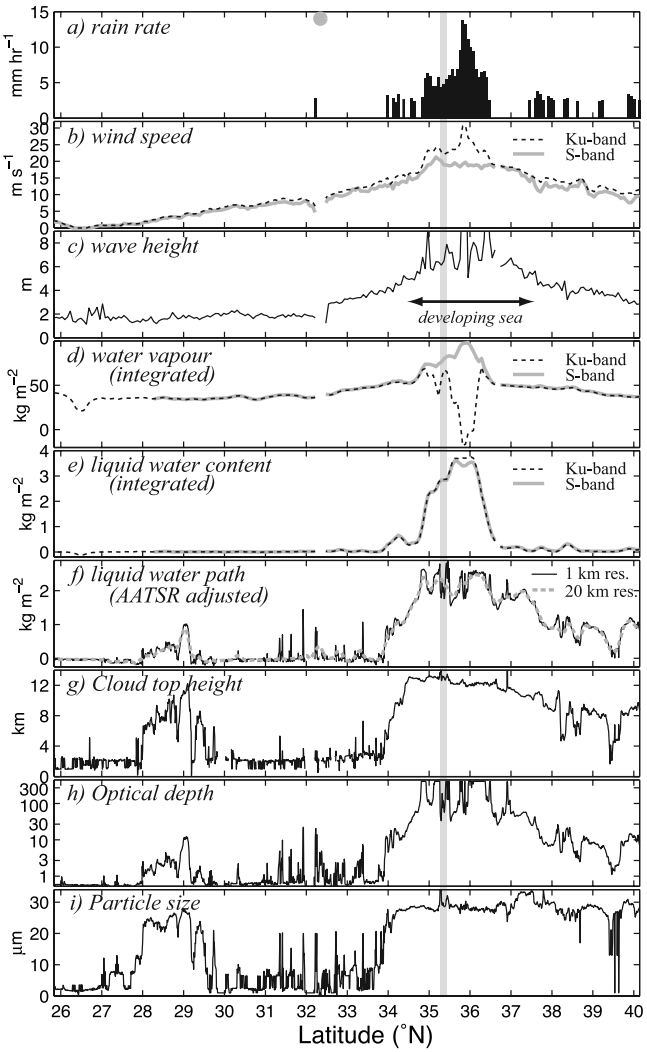


**Figure 3.** Various parameters recorded along nadir track through Hurricane Juan, with the vertical bar at 35.35°N indicating nearest point to hurricane's eye. (a, b, c) Values are derived from RA-2 (light spot at top of Figure 3a indicates latitude of Bermuda, which affects the altimeter). The horizontal bar in Figure 3c denotes region for which seas are developing rather than swell-dominated. (d, e) Information is principally derived from MWR-2; the two curves in each panel reflect the change on using $f(\sigma^0_S)$ rather than $\sigma^0_{Ku}$ as a measure of sea surface roughness in equation 2. (f, g, h, i) Information derived from AATSR, with the light curve in Figure 3f showing the effect of averaging AATSR data over MWR-2 footprint.

lent to CTH > 12 km) with OD of 60–70 and cirrus fraction of ~0.9, consistent with the AATSR data, once allowance is made for the coarser spatial resolution of that MODIS data set. AATSR provides the additional information that particle size in Juan was ~30 $\mu$m, even to the north of Juan where CTH and OD had decreased.

[15] One intriguing difference is between the LWC inferred from the MWR and Liquid Water Path (LWP) derived from AATSR. Although both estimates are based on multi-frequency observations, there are differences in the sensors' sensitivity to droplet size distribution and temperature. In Figures 3e and 3f, LWC drops rapidly to near-zero north of 36°N whereas LWP values decrease more gradually and are still significant at 40°N. It is believed that this is due to the different drop sizes contributing to the estimates of liquid water. Thus it is likely that the remnant feature at 28°–29°N and the high clouds to the north of Juan are principally composed of very fine droplets. The light curve in Figure 3f shows the effect of averaging LWP over corresponding MWR footprint, indicating that the differences from LWC are not merely due to resolution. The unfiltered LWP has much more along-track variation; comparisons with airborne data are needed to determine their reliability.

## 4. Triple Sensor Information

[16] From the altimeter record for Sept/Oct. 2003, we had identified 10 events in the western N. Atlantic, all with heavy rain but minimal contamination by land. Each has been examined as a series of profiles (as in Figure 3); here we bring the contrasting information from all three sensors together using cluster plots. Of those considered, the most informative was a plot of OD against rain rate, classified by MWR-2's LWC (Figure 4). We display the data for Hurricane Juan first, and then the combined data for all 10 events. Rain rates are only calculated if the observed attenuation exceeds 0.5 dB. In the low LWC category (indicated in green) few records have a definite indication of rain, and these do not exceed 4 mm hr$^{-1}$. The highest values of LWC (shown in black) are associated with large values of OD and significant rain. In particular, 'moderate rain' (4–7 mm hr$^{-1}$) requires OD > 6 and LWC > 1, whilst heavy rain needs conditions with OD>30. (These thresholds for the western extra-tropical N. Atlantic are similar to those found in the tropical storm genesis region in the Gulf of Guinea [*Quartly*

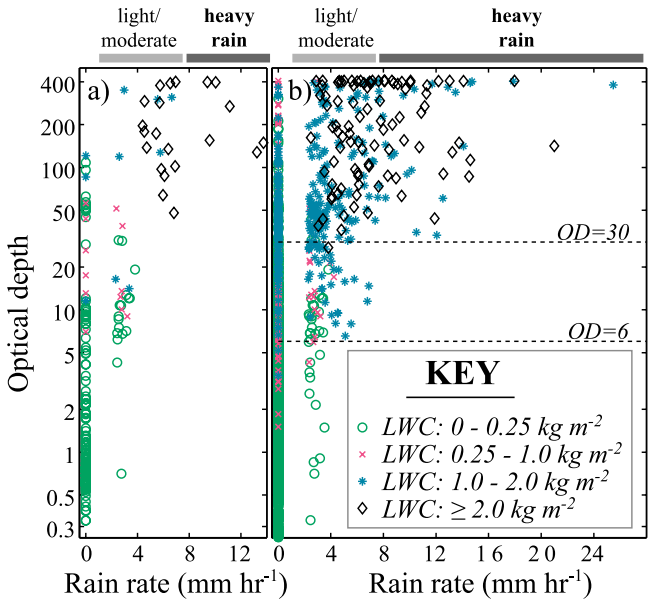


**Figure 4.** Cluster plots linking rain rate to optical depth of clouds, for various values of columnar liquid water content (LWC) from MWR-2. (a) Hurricane Juan alone. (b) Collation of 10 case studies in western N. Atlantic. (Optical depth has been averaged over altimetric footprint. The threshold for RA-2 rain detection corresponds to 2.3 mm hr$^{-1}$.)

*and Poulsen*, 2005].) Measurements from the microwave and infra-red radiometers thus show whether a region has the preconditioning to support light, moderate or heavy rain. However, a given OD and LWC encompass a wide range of actual rainfalls, and thus passive measurements cannot be used to give accurate rainfall on a point-by-point basis, although they may do a good job for an areal average. The cluster plot for Juan alone (Figure 4a) shows that the variability in rain rate for given OD-LWC conditions occurs within individual storms, rather than being due to variations across different rain events.

[17] Results have been shown in terms of rain rate, using a uniform value of 4.5 km for the melting level height, $H$ (equation 1). *Tournadre* [2006] calculates $H$ based on microwave radiometer data, but such is not done here, to avoid MWR-2 data contributing to the altimetry signal, confounding comparisons between all three sensors. Also, in systems with strong updraft, many particles of liquid water may exist above the 0°C isotherm.

## 5. Summary

[18] Altimetry across major storms has been the subject of earlier work, but it is only with *Envisat* that we get an important platform for atmospheric studies, encompassing a dual-frequency altimeter and passive microwave and infra-red radiometers, with each responding to particular components of raining cloud systems. However, little work has been done to-date on bringing these three data records together to provide complementary information. Although somewhat constrained by the nadir-viewing limitation of the radar altimeter and MWR, this suite of multi-frequency sensors can provide significant information relating to active rain systems throughout the globe. In a focussed study on Hurricane Juan, the profiles of wind speed, wave height and water vapour were all found to be centred on 35.8°N, ~50 km north of the nearest point to the eye. The AATSR-derived parameters (Figures 3f, 3g, 3h, and 3i) all show a sharp southern limit to Juan at 34°N, but with elevated values only slowly trailing off to the north. These parameters also show a pronounced response to the decaying remnant at 28°–29°N. Altimetric records of rain extend much further to the north side, an asymmetry confirmed by ground-based and airborne measurements. The asymmetry of surface winds relative to the eye grew only in its later stage as the forward speed of Juan increased.

[19] WV estimates according to the present implementation of the neural net can give aphysical results for storms with significant rain; a simple substitution involving $\sigma^0$ measured at the lower frequency gives much more realistic WV profiles, without adversely affecting data quality elsewhere. However, there is a marked difference in the profiles of liquid water derived from the MWR-2 and AATSR, reflecting their differing responses to small droplets.

[20] The bringing together of all three datasets shows that OD and LWC can be used to give good thresholds on the conditions that may support light, moderate or heavy rain, but that they cannot be used for quantitative determination on a small scale. Thus our study concludes that active radar systems are a prerequisite for satellite studies of rapid spatial variations within storms. However, further analysis of these synoptic measurements, spanning a wider geographical range, may improve the accuracy of areal averages based solely on passive techniques.

[21] **Acknowledgments.** *Envisat* data were provided by ESA under Cat-1 proposal 'Accurate Rain Information from Envisat Sensors,' with AATSR cloud processing by Caroline Poulsen at the Rutherford Appleton Laboratory. We are grateful to Estelle Obligis for providing the neural net code for MWR corrections, and to James Watson for help in implementing it.

## References

Fogarty, C. T., R. J. Greatbatch, and H. Ritchie (2006), The role of anomalously warm sea surface temperatures on the intensity of Hurricane Juan (2003) during its approach to Nova Scotia, *Mon. Weather Rev.*, *134*, 1484–1504.

Goldhirsh, J., and E. J. Walsh (1982), Rain measurements from space using a modified Seasat-type radar altimeter, *IEEE Trans. Antennas Propag.*, *30*, 726–733.

Obligis, E., L. Eymard, N. Tran, S. Labroue, and P. Femenias (2006), First three years of the Microwave Radiometer aboard Envisat: In-flight calibration, processing and validation of the geophysical products, *J. Atmos. Oceanic Technol.*, *23*, 802–814.

Pierson, W. J., and L. Moskowitz (1984), A proposed spectral form for fully-developed wind seas based on similarity theory of S. A. Kitagorodoskii, *J. Geophys Res.*, *69*, 5181–5190.

Quartly, G. D. (1997), Achieving accurate altimetry across storms: Improved wind and wave estimates from C-band, *J. Atmos. Oceanic Technol.*, *14*, 705–715.

Quartly, G. D., and C. A. Poulsen (2005), Coincident cloud observations by altimetry and radiometry, *Eur. Space Agency Spec. Publ.*, *ESA SP-572*, 5 pp.

Quartly, G. D., and M. A. Srokosz (2003), Rain-flagging of the Envisat altimeter, paper presented at International Geoscience and Remote Sensing Symposium, IEEE, Toulouse, France, 21–25 July.

Quartly, G. D., T. H. Guymer, and M. A. Srokosz (2002), Back to basics: Measuring rainfall at sea. part 2: Space-borne sensors, *Weather*, *57*, 363–366.

Quilfen, Y., J. Tournadre, and B. Chapron (2006), Altimeter dual-frequency observations of surface winds, waves, and rain rate in tropical cyclone Isabel, *J. Geophys. Res.*, *111*, C01004, doi:10.1029/2005JC003068.

Tournadre, J. (2006), Improved level-3 oceanic rainfall retrieval from dual-frequency spaceborne radar altimeter systems, *J. Atmos. Oceanic Technol.*, *23*, 1131–1149.

Tournadre, J., and G. D. Quartly (2003), Validation of Envisat RA2 rain flag, *Tech. Rep. DRO-OS 03/01*, 12 pp., IFREMER, Brest, France.

Watts, P. D., C. T. Mutlow, A. J. Baran, and A. M. Zavody (1998), Study on cloud properties derived from Meteosat Second Generation observations, *EUMETSAT ITT 97/181*, EUMETSAT, Darmstadt, Germany.

T. H. Guymer and G. D. Quartly, National Oceanography Centre, Southampton, Empress Dock, Southampton SO14 3ZH, UK. (gdq@noc.soton.ac.uk)